

# A TEM study of the interfaces and matrices of SiC-coated carbon fibre/aluminium composites made by the $K_2ZrF_6$ process

X. CHEN

*Zhejiang Research Institute of Metallurgy, Hangzhou 310013, People's Republic of China*

G. ZHEN, Z. SHEN

*Institute of Metal Research, Academia Sinica, Shenyang 11015, People's Republic of China*

Carbon fibre-reinforced aluminium composites were pressurelessly cast by using  $K_2ZrF_6$  as the wetting promotion agent. Transmission electron microscopy (TEM) and energy dispersed analysis of X-rays, (EDAX) were used. The results showed that interfacial reactions were very active after  $K_2ZrF_6$  treatment. This was caused by the diffusion and reaction of zirconium in the surface of carbon fibres or in the SiC coating. Silicon alloying of aluminium could suppress the interfacial reactions by decreasing the activity of zirconium and changing intermetallic  $Al_3Zr$  to  $Zr_3Al_4Si_5$ , and building up the phase equilibrium between SiC, aluminium and silicon. The requested silicon content was higher than the equilibrium content of Al–Si–SiC system to suppress the SiC/Al interfacial reaction. A perfect interface was achieved in SiC-coated carbon fibre Al–12 wt% Si composite.

## 1. Introduction

Carbon fibre reinforced aluminium composites have attracted considerable interest because of their high potential performance. In fabrication of high-performance materials, two problems have to be resolved, i.e. poor wettability and the reactivity between carbon fibres and aluminium. The first problem makes it hard for aluminium melt to infiltrate into the fibre network completely. The second problem may improve the bonding strength between fibres and matrix, but it will generally damage carbon fibres and decrease the properties of the composites. Many processes have been developed to improve the wettability between carbon fibre and aluminium, such as Na–Sn processing, Ti–B chemical vapour deposition (CVD) coating and metal coatings [1]. Other techniques have been developed to suppress the reaction between carbon fibres and aluminium; for example, SiC and TiC ceramic coatings have been developed [2, 3]. The pressure-casting process was also used [4]. By this means, a great reduction was achieved in the processing temperature and the contact time between aluminium melt and carbon fibres thus reducing the interfacial reaction. It was also very effective to suppress the interfacial reaction by alloying the matrix with silicon, especially in the Al–SiC system [5].

To improve the wettability between carbon fibre and aluminium, a simple processing technique was recently developed, i.e. treating fibres with aqueous  $K_2ZrF_6$  solution [6–8]. By this means, aluminium melt could easily infiltrate into the fibre tow (carbon fibre or SiC fibre). However, the fibre surface was activated because of exothermic reactions between aluminium and  $K_2ZrF_6$ , which resulted in

a great number of  $Al_4C_3$  crystals grown on the fibre surface [9]. It seemed that just one of these techniques was not enough to resolve completely the problems of interfacial compatibility. These techniques should be combined in order to achieve the best results. For example, to suppress the reactions caused by  $K_2ZrF_6$ , carbon fibres were coated with CVD SiC [10].

Interfacial reactions are crucial to the composite properties, and so are extensively investigated. The interface of aluminium graphite fibre with the plasma-enhanced CVD (PECVD) SiC coating was investigated by Li *et al.* [11]. Examination by high-resolution TEM showed that the SiC coating was amorphous. Pressure infiltration of molten aluminium (963 K) into fibres at 621 K resisted interfacial reaction almost completely. In studying the interfacial reactions between SiC and aluminium, no reaction zone was observed in the sintered SiC with a rich Si/Al interface while the formation of  $Al_4C_3$  was observed at the pressureless sintered SiC/Al interface [12]. The SiC/Al interfacial reaction could be suppressed by addition of silicon into the aluminium [13]. Rocher *et al.* [8] studied the reactions in the molten aluminium, carbon and  $K_2ZrF_6$  system. However, the characteristics of the C/Al interface remain undetermined in the  $K_2ZrF_6$  process, as for the SiC/Al interface. The behaviour of silicon in molten aluminium, SiC and  $K_2ZrF_6$  is, so far, unknown.

In this paper, SiC-coated carbon fibre/aluminium (CF/Al) composites were pressurelessly cast using  $K_2ZrF_6$  to promote wetting. The effect of silicon alloying on the interfacial reaction and matrix morphology was investigated.

## 2. Experimental procedure

Fabrication of CF/Al composites included the following steps. First, high-strength PAN-II carbon fibres were continuously coated with an SiC coating by CVD. Second, the SiC-coated carbon-fibres preform was treated with hot aqueous  $K_2ZrF_6$  solution. Then the preform was dried and pressurelessly cast in a mould preheated to 573 K. The temperature of the aluminium or the Al-Si alloy melt was 993 K. The purities of aluminium and silicon used in the experiments were 99.8 wt % and 99.9 wt %, respectively. The size of the composites was 4 mm × 10 mm × 100 mm.

TEM samples were sliced from the composites and ground to a thickness of 20–30 μm, and then ion-thinned at an initial voltage of 5 kV for 2 h at a tilt angle of 20°, and 4 h at 15° respectively, then the voltage was reduced to 4.5 kV and the angle to 12°. The microstructure of the composites was examined on a Philips EM-420 transmission electron microscope (TEM) with a resolution of 0.24 nm. EDAX was also used. The mean spatial resolution diameter was approximately equal to 30 nm.

## 3. Results

### 3.1. CF/Al interface without SiC coating

Fig. 1a shows the interface of uncoated CF/Al composite. The reaction zone at the interface was about 0.3–0.6 μm wide according to the extensive observa-

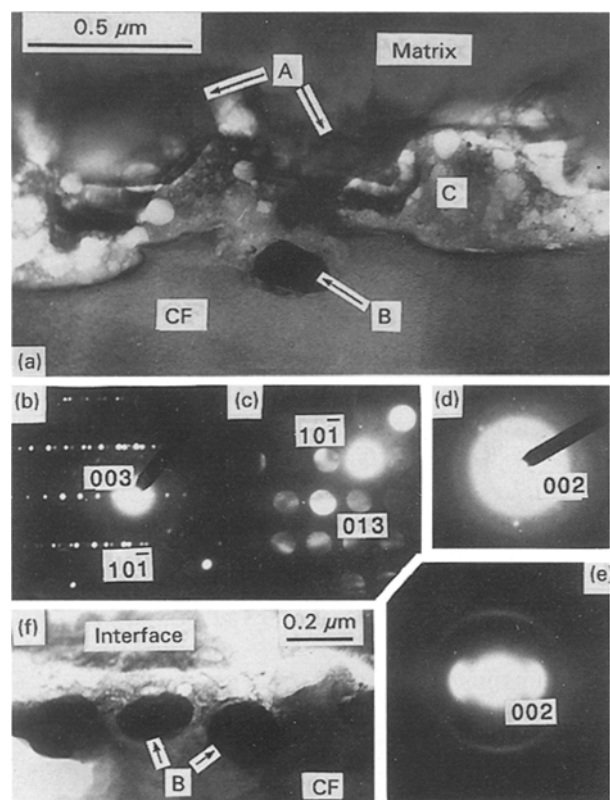


Figure 1 (a) A typical carbon fibre/pure aluminium interface with a very wide reaction zone.  $Al_4C_3$  (A) and  $Al_3Zr$  (B) crystals were detected at the interface. Region C, spreading along the interface was a partially reacted fibre zone. (b–e) Diffraction patterns of  $Al_4C_3$ ,  $Al_3Zr$ , reacted carbon fibre in region C and unreacted carbon fibre, respectively. (f) Another interface region with many  $Al_3Zr$  crystallites in the fibre surface.

tion by TEM. The surface of the carbon fibre had been damaged severely due to interfacial reactions. Reaction between carbon fibres and aluminium resulted in the formation of bulk  $Al_4C_3$  crystals, marked A in Fig. 1a, whose electron diffraction pattern (Fig. 1b) showed the existence of twin crystals. Reaction product B consisted of aluminium and zirconium, and was found to be  $Al_3Zr$  by electron diffraction (Fig. 1c).  $Al_3Zr$  existed extensively in the surface of the carbon fibres. Fig. 1f shows the morphology of  $Al_3Zr$  in another interface zone. The reaction layer, C, consisted of aluminium, potassium, silicon and a small amount of zirconium examined by EDAX. But its electron diffraction pattern (Fig. 1d) indicated that it was mainly composed of carbon. It was for this reason that EDAX could not detect the existence of light elements, such as carbon and fluoride. The main constituent, carbon, was excluded. Apparently, the elements detected by EDAX in this zone were impurities. Compared with that of the intact carbon fibre, the (002) diffraction of layer C changed from satellite stripes (Fig. 1e) to non-crystal rings (Fig. 1d). It indicated that the crystallinity of the carbon fibre decreased after the impurity elements aluminium, potassium, zirconium, etc. diffused into the carbon fibre. Potassium could form intercalated compounds with graphite crystallites of the carbon fibre, such as  $C_8K$ ,  $C_{16}K$ , and resulted in an increase of the interlayer width of the graphite crystallite, and hence a decrease in the crystallinity of the carbon fibre.

### 3.2. Interface of the SiC-coated CF/Al composite

The reaction zone in the CF/Al composite with an SiC coating was much thinner than that of the uncoated composite. Its thickness was about 0.04–0.2 μm, which was about the thickness of the SiC coating. Fig. 2 shows a typical SiC-coated CF/Al interface. No silicon was detected but aluminium and potassium were identified by EDAX on the interface. This indicated that the SiC coating had reacted and the reaction product diffused into the matrix. The crystallites grown at the interface were proved to be  $Al_4C_3$  by their micro-electron diffraction pattern shown in the upper right corner of Fig. 2. Although the SiC coating

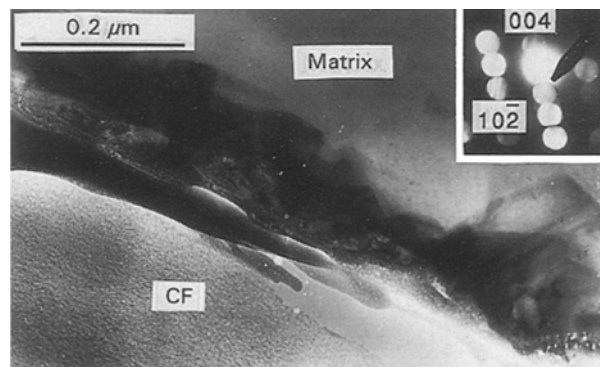


Figure 2 SiC-coated carbon fibre/pure aluminium interface with  $Al_4C_3$  crystals growing from the fibre surface to the matrix. Top right corner: the microdiffraction pattern of (001)\* facet of  $Al_4C_3$ .

had reacted, the carbon fibre was only slightly damaged.

### 3.3. Interfaces of the SiC-coated CF/Al–Si alloy composites

The interfacial reaction could be suppressed to a different extent by alloying the matrices with different amounts of silicon. Fig. 3 shows the interface of the SiC-coated CF/Al–2 wt % Si composite: the SiC coating is seen to have reacted. The reaction product mainly consisted of aluminium, silicon and zirconium, as found by EDAX. This phase was not able to be determined by electron diffraction because the crystals were too small. The product might be  $(\text{AlSiZr})_{8U}$  phase, according to X-ray diffraction analysis of the reaction products of the Al–SiC– $\text{K}_2\text{ZrF}_6$  system [14]. The white zone, A, in the reaction layer mainly consisted of aluminium, the surplus was silicon, potassium and zirconium. Fig. 4 shows another interface region. Although some bulk crystals grew at the interface, the surface of the carbon fibres was not damaged. The phase of these bulk crystals was not determined by electron diffraction. It mainly consisted of aluminium, silicon and a small amount of potassium; it might be a compound of aluminium, silicon and carbon. A sim-

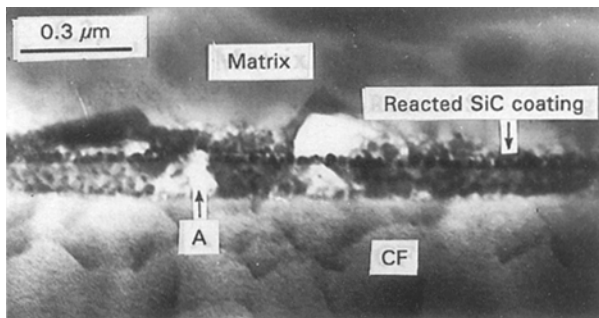


Figure 3 Morphology of the partially reacted SiC coating of the CF/Al–2 wt % Si composite interface.

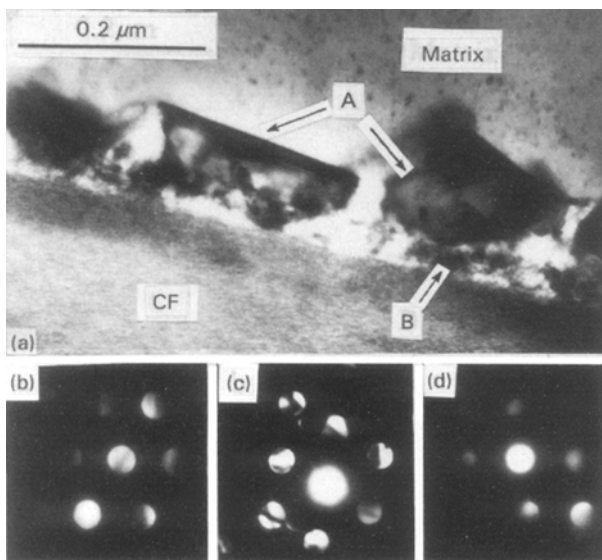


Figure 4 (a) A typical interface of SiC-coated CF/Al–2 wt % Si composite showing the reacted SiC coating and growth of reaction products; (b–d) Microdiffraction patterns of phase A.

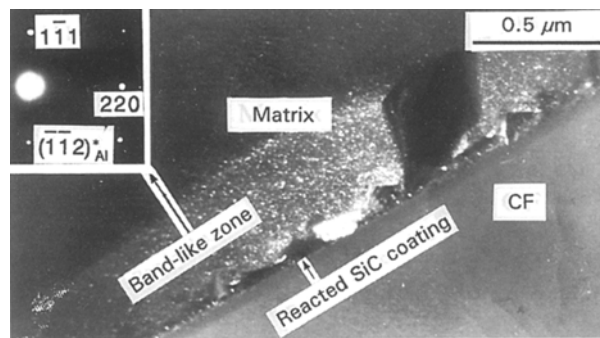


Figure 5 Dark-field image of precipitated silicon in the band-like matrix contiguous to the interface. The diffraction pattern of this zone showed the  $(112)^*$  facet of aluminium.

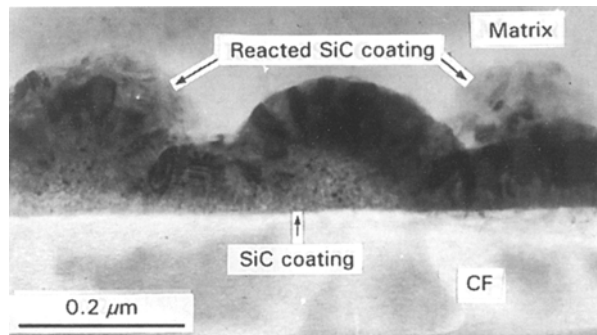


Figure 6 Features of the partially reacted SiC-coated CF/Al–6 wt % Si composite interface.

ilar substance was found at the interface of SiC/Al by Marcus [15].

Fig. 5 is a dark-field image taken at the same region as Fig. 4. The band-like zone dispersed with particles is seen to have a clear boundary with the fibre and the other part of the matrix. Electron diffraction and EDAX showed that this zone of the aluminium matrix contained silicon. A similar phenomenon was also found in a composite with high silicon content.

In Al–6 wt % Si matrix composite, the interfacial reactions were further suppressed. Fig. 6 shows the interface morphology of this material: only a small part of the SiC coating is seen to have reacted. Fig. 7a shows another interface region; no reaction is seen between matrix and SiC coating. Silicon crystals segregated on the coating, as shown by the electron diffraction pattern in Fig. 7b. Interfaces of CF/Al–12 wt % Si composite showing intact SiC coating are seen in Fig. 8. More silicon had segregated along the interface.

Electron diffraction patterns proved that the coating made by CVD was  $\beta$ -SiC as shown in Fig. 7c and d. The diffraction ring in Fig. 7c indicated that the coating near the fibre was polycrystalline, while the outer layer was well-ordered crystallite as the diffraction pattern showed in Fig. 7d. The SiC coating in Figs 6 and 7 was very thick, because this sample was specially prepared to determine the structure of the SiC coating. It could be concluded that the SiC coating grew in a disorderly manner on the surface of the carbon fibres at the beginning of deposition. Then it

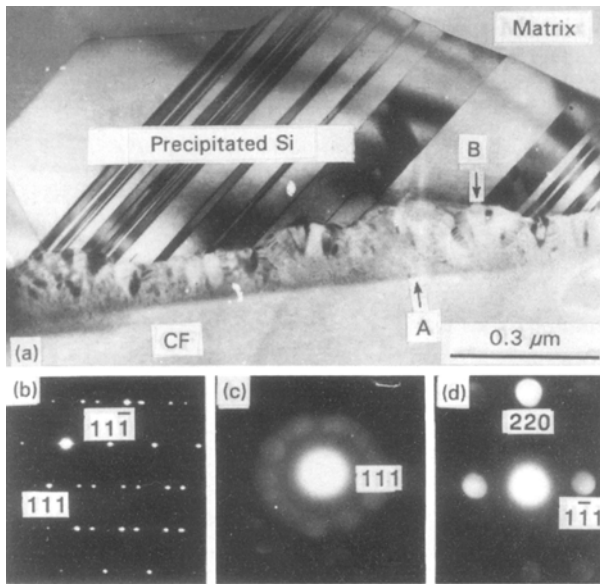


Figure 7 (a) The morphology of the precipitated silicon crystal at the interface of the SiC-coated CF/Al-6 wt % Si composite and (b) its diffraction pattern; (c, d) microdiffraction patterns of the SiC coating corresponding to regions A and B, respectively.

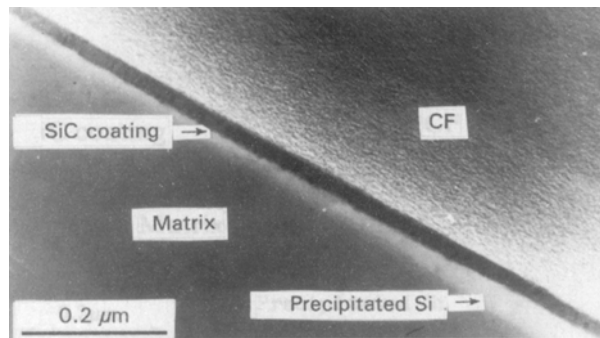


Figure 8 Features of the intact interface with a thin silicon layer precipitated on the CF/Al-12 wt % Si composite.

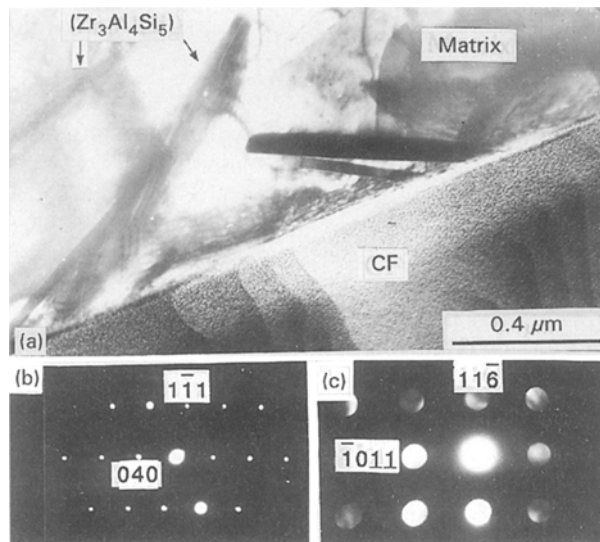


Figure 9 (a) Morphology of the precipitated  $Zr_3Al_4Si_5$  on the interface; (b, c) the diffraction patterns of this phase.

grew along the lower-energy lattice plane, and developed into a cone-like crystallite.

Interfacial structure may be perceived further in Fig. 9 showing CF/Al-12 wt % Si composite. Inter-

metallic  $(Zr_3Al_4Si_5)_{24U}$  is seen to have precipitated on the interface. Fig. 9b and c are the diffraction patterns of the intermetallics. Although the SiC coating was very thin at the interface, no evidence of interfacial reaction was found.

### 3.4. Morphology of the matrix in composites

Fig. 10 shows the morphology of pure aluminium matrix in the composite. The rod-like and bulk substances were found to be  $Al_3Zr$  by electron diffraction. The  $Al_3Zr$  phase also existed in the matrix of CF/Al-2 wt % Si composite. No other intermetallic compounds were found in the low-silicon content matrix.

Fig. 11 shows the morphology of the precipitated phase in Al-12 wt % Si alloy matrix. The bulk and

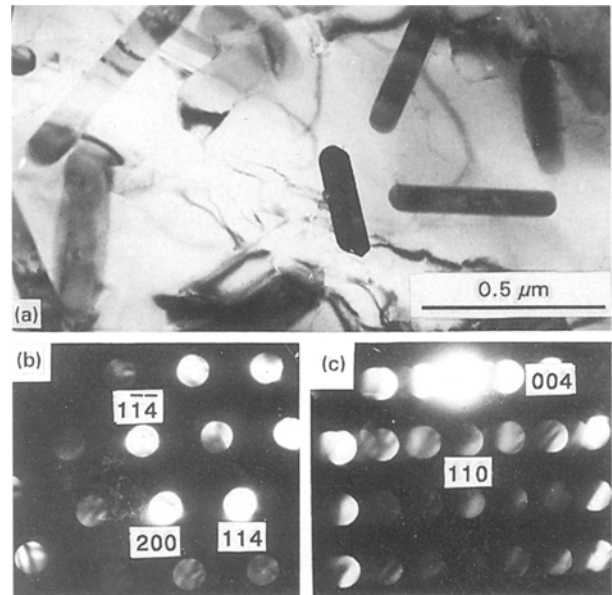


Figure 10 (a) Features of the carbon fibre/pure aluminium composite matrix showing existence of  $Al_3Zr$ . (b, c) The diffraction patterns of  $Al_3Zr$ .

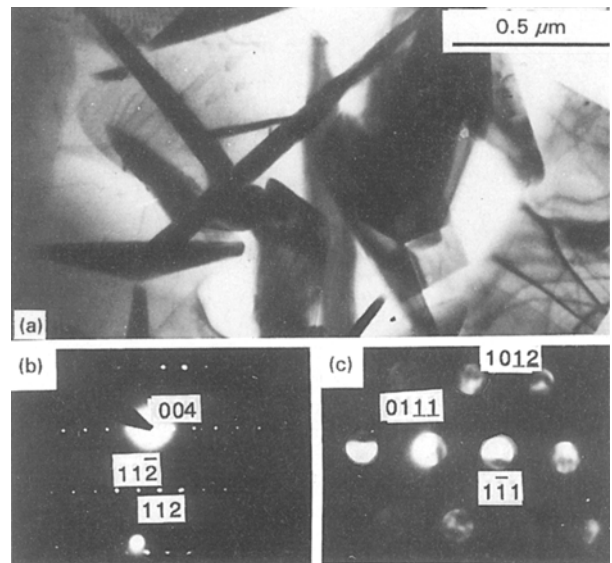


Figure 11 (a) Features of the CF/Al-12 wt % Si composite matrix showing the existence of  $Zr_3Al_4Si_5$ . (b, c) The diffraction patterns of  $Zr_3Al_4Si_5$ .

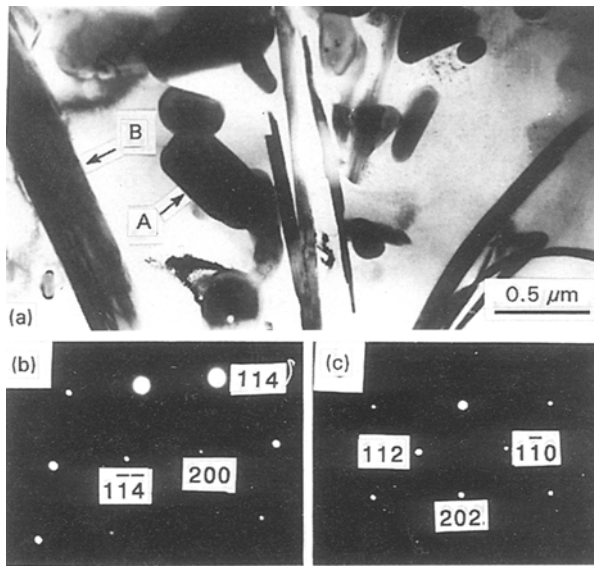


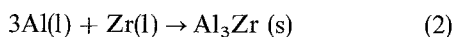
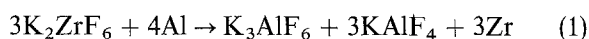
Figure 12 (a) Features of the CF/Al-6 wt % Si composite matrix showing the co-existence of  $\text{Al}_3\text{Zr}$  (A) and  $\text{Zr}_3\text{Al}_4\text{Si}_5$  (B). (b, c) The diffraction patterns of  $\text{Al}_3\text{Zr}$ .

needle-like substance was proved to be  $(\text{Zr}_3\text{Al}_4\text{Si}_5)_{24\text{U}}$  as in Fig. 9. No other phases were found, including free silicon. The morphology of the precipitated phase in the Al-6 wt % Si alloy matrix is shown in Fig. 12. There were two precipitated phases. EDAX and electron diffraction showed that the bulk, blunt phase was  $\text{Al}_3\text{Zr}$ , and the long, thin phase was  $\text{Zr}_3\text{Al}_4\text{Si}_5$ .

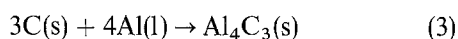
From the above three figures, it could be seen that the existing form of zirconium changed from  $\text{Al}_3\text{Zr}$  to  $\text{Zr}_3\text{Al}_4\text{Si}_5$  when more silicon was added. Obviously, this was caused by a high concentration of silicon in the matrix. A small amount of silicon (2 wt %) did not have this effect, because it mainly dissolved in the matrix. For a higher silicon content (6 wt %) matrix, although part of the silicon was still dissolved in the matrix, the surplus would react with aluminium and zirconium. Therefore, two phases, i.e.  $\text{Al}_3\text{Zr}$  and  $\text{Zr}_3\text{Al}_4\text{Si}_5$  co-existed in the Al-6 wt % Si alloy matrix. When the matrix silicon content reached 12 wt %, it was high enough to change  $\text{Al}_3\text{Zr}$  into  $\text{Zr}_3\text{Al}_4\text{Si}_5$ . It seems that  $\text{Zr}_3\text{Al}_4\text{Si}_5$  is a more stable phase than  $\text{Al}_3\text{Zr}$ .

#### 4. Discussion

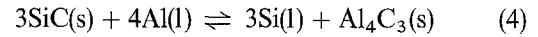
Because  $\text{K}_2\text{ZrF}_6$ , SiC coating and silicon were brought into the interface of the CF/Al composite, the interfacial behaviour became very different and complex. Rocher *et al.* [8] studied the wetting improvement mechanism between C and Al by the  $\text{K}_2\text{ZrF}_6$  process, and proposed that the following reactions took place in this system



These were exothermic reactions, so that they activated the reaction between carbon fibre and aluminium



The reaction product  $\text{Al}_4\text{C}_3$ , was observed at the interface by TEM (see Figs 1 and 2). When the SiC coating was induced at the interface, a diffusion barrier was set up between carbon fibres and aluminium so that Reaction 3 was suppressed. As a result, it prevented the carbon fibres from being damaged, while the reaction zone became much smaller. However, the SiC coating was still itself reacted. Generally, the reactivity between SiC and aluminium was low at the temperature of fabrication of composites compared with the results of Li [11]. It was certain that  $\text{K}_2\text{ZrF}_6$  also activated the reaction between SiC and aluminium



The interfacial reaction might be suppressed to a different extent by the addition of silicon to the molten aluminium (see Figs 2 and 3). Viala *et al.* [16] studied the phase equilibrium and chemical interaction in the Al-Si-SiC system and pointed out that SiC could be stable in molten aluminium when a proper quantity of silicon was added. The equilibrium silicon content was about 5 wt % at temperature of 1000 K. According to his result, there should be no interfacial reaction in CF/Al-6 wt % Si composite. Unfortunately, part of the SiC coating was still reacted, as shown in Fig. 6. Our previous X-ray diffraction analysis proved that the reaction



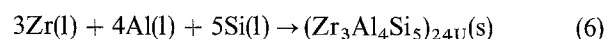
took place in the Al-SiC- $\text{K}_2\text{ZrF}_6$  system [14]. Hence, even if the silicon reached the equilibrium content of the Al-Si-SiC system, part of the SiC coating would still be sacrificed to react with zirconium.

In summary, when  $\text{K}_2\text{ZrF}_6$  existed, it could be concluded that

(a) at the CF/Al interface, the primary interfacial reaction was Reaction 3. The diffusion and reaction of the products of Reaction 1 in the fibre surface were also very active. As pointed out above,  $\text{Al}_3\text{Zr}$  crystals grew in the surface of the carbon fibre, and the crystallinity of the surface carbon decreased (see Fig. 1). All these phenomena strongly supported our conclusion;

(b) at the SiC/Al interface, the primary interfacial reactions were Reaction 4 and 5. Reaction 4 can be suppressed by silicon alloying. Reaction 5 can be suppressed by reducing the activity of zirconium in the liquid phase because the products are all in solid form. It seems that Reaction 2 might be a possible way of decreasing the activity of zirconium. However, the SiC coating was reacted when some  $\text{Al}_3\text{Zr}$  existed in the matrix. It was probable that the Gibbs' enthalpy of Reactions 2 and 5 were at the same level. Reaction 2 would not predominate and would be invaluable in resisting Reaction 5.

In studying the CF/Al-Si composite, the intermetallic  $\text{Zr}_3\text{Al}_4\text{Si}_5$  was found. This indicated that the reaction:



probably took place. Zirconium would preferentially react with silicon and aluminium, and give  $\text{Zr}_3\text{Al}_4\text{Si}_5$ . As a result, not only was Reaction 4 suppressed, but

also the activity of zirconium in the liquid phase was reduced by silicon alloying. The interfacial reactions were suppressed gradually with increasing silicon content in the aluminium melt. Intact SiC coating was preserved in the CF/Al-12 wt % Si composite. The form of zirconium changed from  $\text{Al}_3\text{Zr}$  to  $\text{Zr}_3\text{Al}_4\text{Si}_5$  in accordance with this. Silicon could effectively prevent the chemical reaction at the SiC/Al interface.

## 5. Conclusions

1. In the  $\text{K}_2\text{ZrF}_6$  treatment process, interfacial reactions were very severe in the uncoated CF/Al composite. The SiC coating could prevent the reactions between carbon fibres and aluminium, but it reacted with itself. Severe interfacial reactions were brought about by the diffusion of the products of Reaction 1, especially for zirconium and potassium.

2. Silicon alloying of the matrices could suppress the SiC/Al interfacial reactions by building up the phase equilibrium between aluminium, silicon and SiC, and decreasing the activity of zirconium, giving intermetallic  $\text{Zr}_3\text{Al}_4\text{Si}_5$ . A perfect interface was achieved in SiC-coated CF/Al-12 wt % Si composite.

3. Zirconium existing in the form of  $\text{Al}_3\text{Zr}$  in the low silicon content composites, while it changed to  $\text{Zr}_3\text{Al}_4\text{Si}_5$  with increasing silicon content.

## References

1. M. F. AMATEAU, *J. Compos. Mater.* **10** (1976) 279.

2. K. HONJO and A. SHINDO, *Yogyo Kyokai Shi* **94** (1986) 172.
3. L. AGGOUR, E. FITZER, E. IGNOTOWITZ and M. SAHEBKAR, *Carbon* **12** (1974) 358.
4. A. MARTENSEN, J. A. CORINE and M. C. FLEMINGS, *J. Metals* **2** (1988) 13.
5. M. K. SHORSHOROV, T. A. CHERNYSHOVA and L. I. KOBELEVA, in "Progress in Science and Engineering of Composites", edited by T. Hayashi, K. Kawata and S. Umekawa, ICCM IV, Tokyo (Japanese Society for composite Materials, 1982) p. 1273.
6. J. P. ROCHER, J. M. QUENISSET and R. NASLAIN, *J. Mater. Sci. Lett.* **4** (1985) 1527.
7. *Idem.*, US Pat. 4659 593, 21 April 1987.
8. *Idem.*, *J. Mater. Sci.* **24** (1989) 2697.
9. S. SCHAMM, J. P. ROCHER and R. NASLAIN, in "Development in Science and Technology of Composite Materials" (ECCM-3), European Association for Composite Materials, ed. by A. R. Bunsell P. Lamicq. A. Massiah, pp. 157-63.
10. X. CHEN, G. ZHENG, Z. SHEN and H. DU, *Acta Metall. Sinica* **28B** (1992) 180.
11. Q. LI, J. MCGUSAR, L. T. MASUR and J. A. CORNIC, *J. Mater. Sci. Eng.* **A117** (1989) 199.
12. T. ISEKI, T. KAMEDA and T. MARUYAMA, *J. Mater. Sci.* **19** (1984) 1692.
13. H. LU, U. MEDALENO, T. SHINODA, Y. MISHIMA and T. SUZUKI, *ibid.* **25** (1990) 4247.
14. X. CHEN, Z. SHEN and G. ZHENG, *Acta Metall. Sinica* **29B** (1993) 377 (in Chinese).
15. H. L. MARCOUS, AD-A 127590 (1976).
16. J. C. VIALA, P. FORTIER and J. BOUIX, *J. Mater. Sci.* **25** (1990) 1842.

Received 8 August

and accepted 21 December 1995